0023-6837/01/8106-833$03.00/0
LABORATORY INVESTIGATION
Copyright © 2001 by The United States and Canadian Academy of Pathology, Inc.
Vol. 81, No. 6, p. 833, 2001
Printed in U.S.A.

Rb and TP53 Pathway Alterations in Sporadic and NF1-Related Malignant Peripheral Nerve Sheath Tumors

Sarah Birindelli, Federica Perrone, Maria Oggionni, Cinzia Lavarino, Barbara Pasini, Barbara Vergani, Guglielmina N. Ranzani, Marco A. Pierotti, and Silvana Pilotti

Pathology and Cytopathology Unit (SB, FP, MO, CL, BV, SP), Preventive Medicine Unit (BP), and Department of Experimental Oncology (MAP), Istituto Nazionale per lo Studio e la Cura dei Tumori, Milan and Department of Genetics and Microbiology (GNR), University of Pavia, Pavia, Italy

SUMMARY: Karyotypic complexities associated with frequent loss or rearrangement of a number of chromosome arms, deletions, and mutations affecting the *TP53* region, and molecular alterations of the *INK4A* gene have been reported in sporadic and/or neurofibromatosis type I (NF1)-related malignant peripheral nerve sheath tumors (MPNSTs). However, no investigations addressing possible different pathogenetic pathways in sporadic and NF1-associated MPNSTs have been reported. This lack is unexpected because, despite similar morphologic and immunophenotypic features, NF1-related cases are, by definition, associated with *NF1* gene defects. Thus, we investigated the occurrence of *TP53* and $p16^{INK4A}$ gene deregulation and the presence of microsatellite alterations at markers located at 17p, 17q, 9p21, 22q, 11q, 1p, or 2q loci in MPNSTs and neurofibromas either related (14 cases) or unrelated (14 cases) to NF1. Our results indicate that, in MPNSTs, $p16^{INK4A}$ inactivation almost equally affects both groups. However, *TP53* mutations and loss of heterozygosity involving the TP53 locus (43% versus 9%), and p53 wild type overexpression, related or not to mdm2 overexpression (71% versus 25%), seem to mainly be restricted to sporadic MPNSTs. In NF1-associated MPNSTs, our microsatellite results are consistent with the occurrence of somatic inactivation by loss of heterozygosity of the second *NF1* allele. (*Lab Invest 2001, 81:833–844*).

Malignant peripheral nerve sheath tumors (MPNSTs) encompass a wide group of neoplasms with Schwann cell differentiation features. They arise either sporadically or in association with neurofibromatosis type 1 (NF1). Immunocytochemical (ICC) (Kindblom et al, 1995) and karyotypic (Fletcher et al, 1999) investigations have found a recurrent p53 protein overexpression and losses or rearrangements at several chromosomal arms in MPNSTs not otherwise specified. Comparative genomic hybridization studies highlighted gains and losses at a number of chromosomal regions affecting both NF1-related and -unrelated MPNSTs (Mechtersheimer et al, 1999). Mutational analyses restricted to a few NF1-related MPNSTs showed *TP53* mutations (Legius et al, 1994; Menon et al, 1990). More recently, alterations of the *INK4A* gene encoding two distinct growth inhibitors, $p16^{INK4A}$ and $p19^{ARF}$, were reported in 75% and 60% of MPNSTs (Berner et al, 1999; Kourea et al, 1999), irrespective of their belonging to sporadic or NF1-associated cases, and in 50% of NF1-related MPNSTs (Nielsen et al, 1999). Neither *INK4A* gene alterations nor *TP53* mutations have been reported in neurofibromas, and there is contrasting data for p53 protein expression and the occurrence of chromosomal region losses in neurofibromas (Kourea et al, 1999; Menon et al, 1990; Nielsen et al, 1999; Ottini et al, 1995).

Preclinical in vivo models indicate that *ARF*/*p53*-null mice are prone to develop sarcomas and lymphomas (Kamijo et al, 1999), and that inactivation of both the *NF1* and *TP53* genes is required for the malignant conversion of neurofibromas to MPNSTs (Cichowski et al, 1999; Vogel et al, 1999).

Despite similar morphologic and immunophenotypic features, NF1-related and -unrelated MPNSTs differ in clinical and molecular settings. According to a recent population-based clinical and genetic study (Poyhonen et al, 1997), the risk for NF1 patients to develop MPNSTs is 3% and the apparent malignant transition of MPNSTs from neurofibroma is higher in NF1 cases compared with sporadic cases (81% versus 41%, respectively) (Ducataman et al, 1986). At the molecular level, it is assumed that the inactivation of the *NF1* gene, whose product displays a GTPase enzymatic activity, leads to the constitutive activation of the *RAS* oncogene in NF1-related cases (Shen et al, 1996). Because it is unlikely that the loss of *NF1* gene function represents the unique molecular lesion in these malignancies, a role of *INK4A* gene inactivation

Received February 12, 2001.
This work was supported by grants from AIRC/FIRC (Associazione and Fondazione Italiana per la Ricerca sul Cancro).
Address reprint requests to: Dr. Silvana Pilotti, Unita' di Anatomia e Istologia Patologica e Citopatologia, Istituto Nazionale per lo Studio e la Cura dei Tumori, Via G. Venezian, 1, 20133 Milano, Italy. E-mail: pilotti@istitutotumori.mi.it

in malignant transformation has recently been stressed (Nielsen et al, 1999).

However, in the tumorigenesis of sporadic and NF1-associated MPNSTs, *TP53* and *p16*^{INK4A} loss of function has not yet been addressed comparatively. We therefore investigated a series of sporadic and NF1-related cases to define possible pathways of malignant transformation that differed between the two groups. In a series of 28 cases of both MPNSTs and/or neurofibromas, subdivided into 14 NF1-related and 14 NF1-unrelated cases, we analyzed the structural and functional alterations of the *p16*^{INK4} and *TP53* genes, and the immunophenotypic expression of their relative products, p16, p53, and a series of cell-cycle related proteins (pRb and cdk4 for *Rb* pathways and mdm2 for *TP53* pathways, respectively). Additionally, we studied the occurrence of loss of heterozygosity (LOH) and/or microsatellite instability (MSI) at 16 polymorphic loci located at the 17p, 17q, 9p21, 22q, 11q, 1p, and 2q chromosomal regions.

Results

ICC

Details of the ICC data are reported in Tables 1 and 2. p53 immunoreactivity was observed in 4 of 12 (33%) NF1-related MPNSTs and in 7 of 14 (50%) sporadic MPNSTs (Figs. 1a and 2), whereas two mdm2-immunoreactive cases were detected within each group (NF1: 2 of 12, 17%; sporadic: 2 of 14, 14%). No immunoreactivity was identified for p53 or mdm2 in neurofibromas.

p16 immunoreactivity was present in only 1 of 11 (9%) NF1-related case (Table 1, Case 10) and in no sporadic MPNSTs (Table 2, Fig. 1b); whereas all but two neurofibromas (Cases 2 and 15) had p16 immunoreactivity (Fig. 3d). Consistently positive Rb immunoreactivity was observed in all MPNST (Figs. 1c and 3c), whereas neurofibromas were positive at low levels, in keeping with a constitutive expression of pRb and its cell-cycle dependent inactivation by phosphorylation. With the exception of Case 18, no overexpression of cdk4 was detected.

Microsatellite Analysis

All of the lesions included in the study and the corresponding normal tissue were screened for 16 microsatellite loci located at chromosomes 17, 22, 9, 1, 11, and 2. With one exception (Case 16), no LOH was found in neurofibromas (data not shown). The neurofibroma positive for LOH at the D9S171 and D11S905 loci corresponded to a wide re-excision performed at our institute of a primary MPNST that was surgically treated elsewhere 1 month earlier. Interestingly, the MPNST recurrence, analyzed by us 6 years later (Case 16), had the same LOH pattern of neurofibroma at the D11S905 marker.

The results of microsatellite analysis in MPNSTs is summarized as follows (Fig. 4). MPNSTs from NF1 patients had a similar or greater, but not statistically significant, percentage of LOH in almost all loci applied with respect to the sporadic cases, with the exception of the 17p13 locus. The results of the analysis at the 17p13 locus are reported below in detail in "LOH and MSI correlations" in the "*TP53*" section. The *NF1* gene locus is highly involved in NF1 MPNSTs in terms of frequency and of extension of chromosome 17 involvement. In detail, of the 4 cases carrying LOH at the 17q11.2 locus, three of seven cases, 43% (Cases 2, 7, and 8), were NF1-related and one of nine cases, 11% (Case 19) was sporadic. Critical loci harboring relevant tumor suppressor genes or oncogenes such as *NF2*, *p16*^{INK4A}, and *L-Myc* seemed to be involved in both groups of MPNSTs. Finally, MSI played a weak role in both neurofibroma and MPNSTs because it was only occasionally found (data not shown).

TP53

Molecular Analysis. Molecular analysis of *TP53* at exons 5 to 8 was performed successfully in 27 (13 NF1 and 14 sporadic cases) of 28 cases, one case (Case 5) was not evaluable. Seven of the tested tumors had an abnormal single-strand conformation polymorphism (SSCP) pattern; in all of these cases, the presence of a somatic mutation was confirmed by direct sequencing. *TP53* mutations were found in only 1 of 11 NF1 MPNSTs (9%) (Table 1) and in 6 of 14 sporadic MPNSTs (43%) (Table 2), although the statistical analysis was not significant (Fisher-Exact test, $p = 0.118$). Details of the identified genetic changes are reported in Tables 2 and 3.

The exons involved and the frequencies of the mutations were distributed as follows: the mutation found in NF1 cases was located in exon 8, whereas, in sporadic cases, one mutation was identified in exon 5, one in exon 6, two in exon 7, and two in exon 8. Missense mutations resulting in an amino acid substitution were detected in all but one mutated case (case 27) and included one transversion (T:G–G:A), in the NF1 case, and five transitions (G:C–A:T in three cases and A:T–G:C in two cases) in the sporadic cases (Fig. 1d). The remaining mutated case (case 27) carried a base deletion (exon 5, codon 176), which leads to the appearance of a premature stop codon, resulting in an early chain termination during translation. None of the six amino acid substitutions detected in our series occurred in *TP53* mutational hot-spot codons (Greenblatt et al, 1994), although, in all but one case (Case 21), they were located in evolutionary highly conserved regions (Cho et al, 1994; Prives, 1994). None of these codons contained CpG nucleotides.

In Cases 15 and 19, the molecular analysis was extended to exons 4, 9, and 10 because no mutations were observed in exons 5 through 8 despite strong immunoreactivity in more than 90% of the nuclei. Case 15 revealed a *TP53* polymorphism at exon 4, codon 72 (May and May, 1999). In Case 19, *TP53* molecular analysis of exons 4 and 9 was not evaluable and no mutation was identified in exon 10.

ICC Correlation. Overall, p53 ICC overexpression correlated poorly with the *TP53* mutation profile

Table 1. NF1-Related Cases: Clinical-Pathologic and Immunophenotypic-Molecular Data

Case	Lesion	Sex/Age at onset	Familiarity	Site	TP53	p53	mdm2	p16 gene				p16	pRb	cdk4
								ex1	ex2a	ex2b	ex3			
1	MPNST G3	m/16	pos (paternal)	pelvic region	Mut ex8, Cys277Gly	+(90%)	−	N	HD	N	N	−	+	−
1	MPNST G3#			sacral region	Mut ex8, Cys277Gly	+(90%)	−	n/e	n/e	N	N	−	+	−
1	NFB			pelvic region	wt	−	−	N	N	N	N	+	+	−
2	MPNST G2#	f/9	apparently neg	left shoulder	wt	+(30%)	+(30%)	HD	n/e	HD	n/e	−	+	−
2	NFBp			left shoulder	wt	−	−	n/e	n/e	N	N	+	+	−
2	NFBp			paravertebral cervical region	wt	−	−	N	N	N	N	−	+	−
3	MPNST G3	f/26	apparently neg	left thigh	wt	−	−	n/e	n/e	N	N	−	+	−
3	MPNST G3			left thigh	wt	−	−	N	HD	N	N	−	+	−
3	NFB			left thigh	wt	−	−	n/e	n/e	n/e	n/e	+	+	−
4	MPNST G3	f/39	apparently neg	paravertebral region	wt	−	−	N	n/e	N	N	−	+	−
4	NFB			paravertebral region	wt	−	−	n/e	n/e	N	N	+	+	−
5	MPNST G3	m/12	apparently neg	right arm	n/e	−	−	n/e	n/e	n/e	n/e	n/e	n/e	−
6	MPNST G3	f/32	pos (paternal)	right thigh	wt	+(30%)	−	n/e	n/e	N	n/e	−	+	−
7	MPNST G3	m/29	neg	popliteal region	wt	+(30%)	+(30%)	N	HD	N	N	−	+	−
7	MPNST G3			paravertebral region	wt	−	−	N	N	N	N	−	+	−
7	MPNST G3e			popliteal region	wt	−	−	n/e	n/e	n/e	N	−	+	−
8	MPNST G3	f/19	neg	lung	wt	−	−	n/e	N	N	N	−	+	−
9	NFB	f/22	unknown	left arm	wt	−	−	N	N	N	N	+	+	−
10	MPNST G3	m/14	apparently neg	left foot	wt	−	−	n/e	n/e	N	N	+	+	−
10	MPNST G3			left foot	wt	−	−	n/e	n/e	n/e	N	+	+	−
10	NFB			left foot	wt	−	−	n/e	n/e	n/e	n/e	+	+	−
10	NFB			left foot	wt	−	−	n/e	n/e	n/e	n/e	n/e	n/e	−
11	MPNST G3#	m/12	apparently neg	right thigh	wt	−	−	n/e	n/e	n/e	n/e	−	+	−
11	NFBp			right thigh	wt	−	−	n/e	n/e	n/e	n/e	+	+	−
12	MPNST G3	f/31	unknown	pelvic region	wt	−	−	N	N	n/e	N	−	+	−
13	MPNST G3	f/23	apparently neg	right arm	wt	−	−	N	HD	HD	N	−	+	−
13	NFB			right arm	wt	−	−	N	N	N	N	+	+	−
14	NFB	f/15	apparently neg	breast skin	wt	−	−	n/e	N	n/e	N	+	+	−
14	NFB			flank skin	wt	−	−	N	n/e	N	N	+	+	−
14	NFB			shoulder skin	wt	−	−	n/e	n/e	N	n/e	+	+	−
	MPNSTs pos				1/11 9%	4/12 33%	2/12 17%		5/10 50%			1/11 9%		

MPNST, malignant peripheral nerve sheath tumor; NFB, neurofibroma; G, sarcoma grading; #, chemotherapy treatment; p, plexiform in subtype; e, epithelioid in subtype; f, female; m, male; pos, positive; neg, negative; Mut, TP53 mutation; wt, wild type; +, positive; −, negative; N, normal; HD, homozygous deletion; n/e, not evaluable.

Table 2. Sporadic Cases: Clinical-Pathologic and Immunophenotypic-Molecular Data

Case	Lesion	Sex/ Age at Onset	Familiarity	Site	TP53	p53	mdm2	p16 gene				p16	pRb	cdk4
								ex1	ex2a	ex2b	ex3			
15	MPNST G2	f/82	unknown	right forearm	Polym ex4, Arg72Pro	+(90%)	−	HD	n/e	n/e	N	−	+	−
15	NFB			right forearm	wt	−	−	N	N	N	N	−	+	−
16	MPNST G3	f/61	neg	chest region	Mut ex8, Val274Ala	−	−	n/e	N	N	N	−	+	−
16	NFB			chest region	wt	−	−	N	n/e	n/e	n/e	+	+	−
17	MPNST G2	m/25	neg	left thigh	wt	+(20%)	−	n/e	n/e	N	n/e	−	+	−
17	MPNST G2#			lung	wt	+(30%)	−	n/e	HD	N	N	−	+	n/e
18	MPNST G2e	m/37	father: myeloma	popliteal region	Mut ex7, Cys238Tyr	+(50%)	+(50%)	n/e	n/e	n/e	n/e	−	+	+
18	MPNST G2#			lung	Mut ex7, Cys238Tyr	+(50%)	+(50%)	n/e	HD	N	n/e	−	+	−
19	MPNST G3	m/52	brother: colon ca.	right arm	wt	+(90%)	−	n/e	N	N	N	−	+	−
20	MPNST G2#	m/57	neg	abdomen	wt	+(60%)	−	HD	HD	n/e	n/e	−	+	n/e
21	MPNST G3	f/49	neg	mediastinum	Mut ex6, Tyr220Cys	−	−	n/e	n/e	n/e	n/e	−	+	−
22	MPNST G2	m/53	neg	submandibular region	wt	−	−	n/e	N	n/e	n/e	−	+	−
23	MPNST G2e	m/42	unknown	paravertebral region	wt	+(50%)	−	HD	N	n/e	N	−	+	−
24	MPNST G3#	f/55	neg	submandibular region	Mut ex7, Cys238Tyr	+(30%)	+(30%)	HD	n/e	N	n/e	−	+	−
25	MPNST G3	f/72	brother: hepatic ca	shoulder	wt	−	−	n/e	HD	HD	N	−	+	−
26	MPNST G3	m/66	father: intestinal ca	right forearm	Mut ex8, Glu285Lys	−	−	N	N	N	N	−	+	−
27	MPNST G3	f/33	cervix ca	left leg	Mut ex5, 13207delC	−	−	HD	N	N	n/e	−	+	−
28	MPNST G3	f/69	unknown	left shoulder	wt	−	−	n/e	n/e	N	N	−	+	−
	MPNSTs pos				6/14 43%	7/14 50%	2/14 14%		8/13 62%			0/14 0%		

MPNST, malignant peripheral nerve sheath tumor; NFB, neurofibroma; G, sarcoma grading; #, chemotherapy treatment; p, plexiform in subtype; f, female; m, male; pos, positive; neg, negative; Mut, TP53 mutation; wt, wild type; +, positive; −, negative; polym, polymorphism; N, normal; HD, homozygous deletion; n/e, not evaluable.

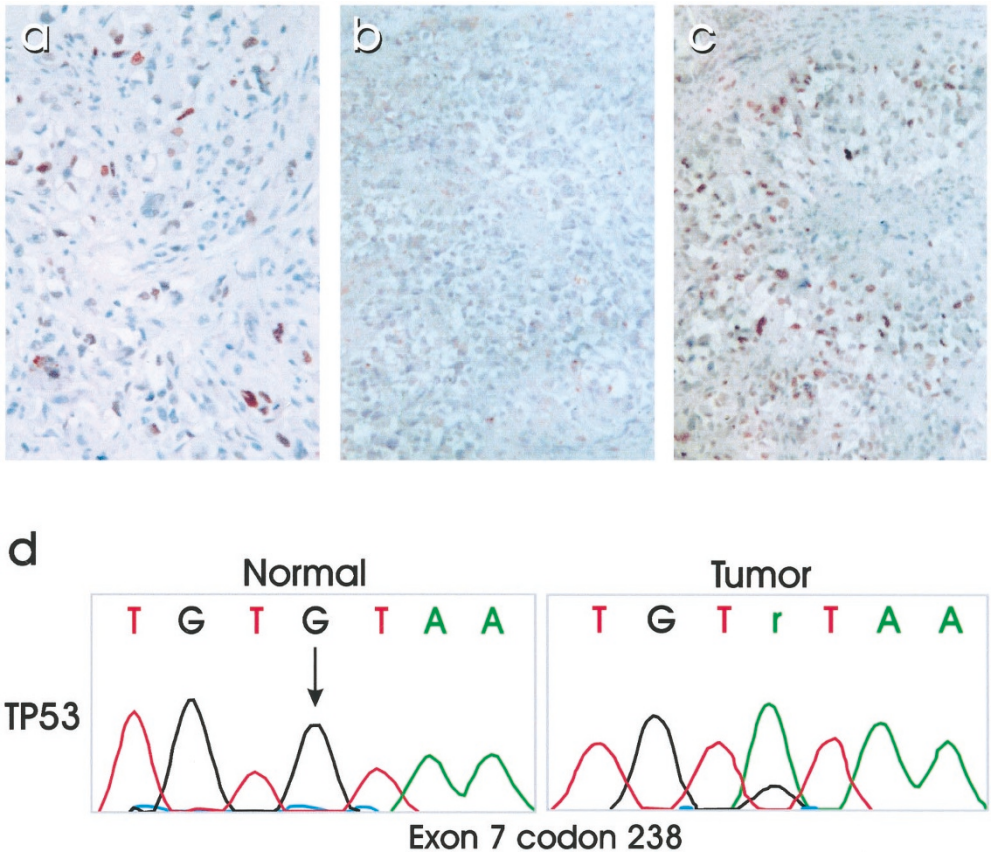

Figure 1.
Immunocytochemical (ICC) and TP53 sequence data of Case 18, sporadic malignant peripheral nerve sheath tumor (MPNST), epitheloid in subtype. a, p53 nuclear expression. b, Loss of p16 expression. c, pRb immunophenotype. d, Nucleotide sequence analysis of a portion of the *TP53* exon 7. The mutated sequence (Cys238Tyr, TGT>TAT) from the *tumor* DNA is compared with the wild-type exon 7 sequence from *normal* control DNA.

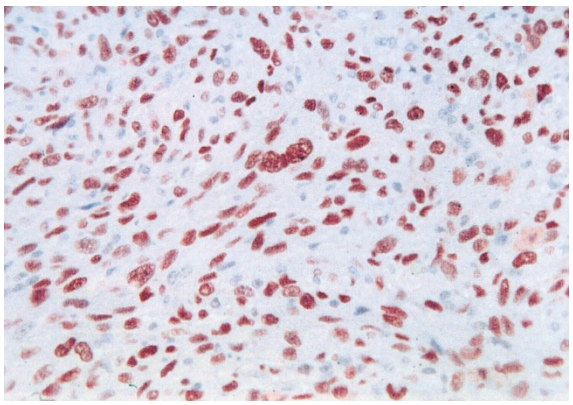

Figure 2.
ICC data of Case 19, sporadic MPNST. Strong p53 immunoreactivity in more than 90% of the nuclei. Despite this ICC profile, no *TP53* mutation was detected in the analyzed exons.

(Tables 1 and 2). In fact, the immunophenotype was consistent with the type of gene mutation in only two cases: Case 1, in which a strong p53 immunoreactivity paralleled the presence of a missense mutation (exon 8, Cys277Gly); and Case 27 with a null immunophenotype and a base deletion (exon 5, codon 176) that generates a premature stop codon determining the synthesis of a truncated protein. In contrast, p53 overexpression not associated with *TP53* mutation nor with mdm2 overexpression was found in one of four (25%) of NF1 and in five of seven (71%) sporadic cases. Interestingly, four of these cases (Cases 15, 19, 20, and 23), had strong p53 immunoreactivity, ranging from 50% to 90% of the nuclei (Fig. 2). Nevertheless, as reported above, no *TP53* mutations were detected in the two cases (Cases 15 and 19) that had p53 immunoreactivity in more than 90% of the nuclei. Furthermore, p53 and mdm2 co-expression was observed in two cases within each group (Cases 2 and 7, and 18 and 24), and was coupled with a wild-type *TP53* in NF1 cases and a mutated *TP53* in the sporadic cases (Tables 1 and 2).

LOH and MSI Correlations. MSI analysis was performed successfully in 25 of 28 cases. LOH at the 17p13 locus was found in two sporadic (2 of 13, 15%) cases (Cases 16 and 18), both carrying a mutated *TP53*, and in one wild-type *TP53* NF1 (1 of 12, 8%) case (Case 4) (Fig. 4). MSI was observed in both the primary tumor and a metastasis in one wild-type *TP53* sporadic case (Case 17) (data not shown).

INK4A

Molecular Analysis. p16^{INK4A} molecular analysis was successfully performed for at least one of three

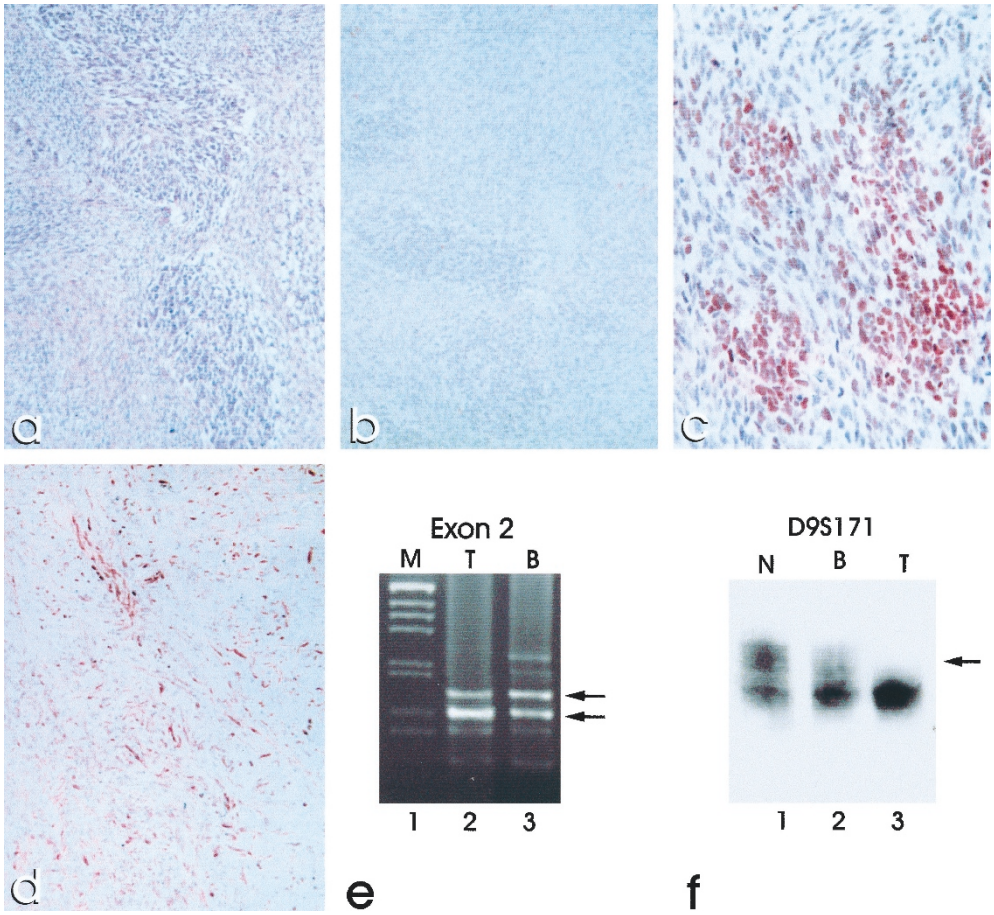

Figure 3.
ICC and molecular data of Case 13, *NF1*-related MPNST (a to c, e to f) and benign peripheral nerve sheath tumor (d to f). MPNST: a, hematoxylin and eosin; b, p16 negativity; and c, pRb immunoreactivity. Neurofibroma: d, p16 immunoreactivity is retained in the benign sample. e, *INK4A* gene molecular analysis shows a homozygous deletion of exon 2 (*upper arrow*) affecting the MPNST (lane 2) but not the neurofibroma (lane 3). The *lower arrow* indicates the DNA band corresponding to the *β-globin* fragment gene co-amplified with the *p16* exon 2. f, Microsatellite data show a partial (lane 2) and a complete (lane 3) loss of the upper allele (*arrow*) of the D9S171 polymorphic marker, whereas the analyzed normal tissue (lane 1) shows both alleles. *M*, 1 kb molecular marker; *T*, MPNST; *B*, neurofibroma; *N*, normal tissue.

exons in 25 of 28 cases (12 NF1 and 13 sporadic cases); three cases (Cases 5, 11, and 21) were not evaluable. Data suggesting a homozygous deletion in MPNSTs were obtained in 5 of 10 (50%) NF1 cases (Table 1) and 8 of 13 (62%) sporadic cases (Table 2); overall, in 13 of 23 (56.5%) MPNSTs.

In detail, deletions of *p16*^{INK4A} exon 1 were observed in 1 of 7 (14%) NF1 cases and 5 of 6 (83%) sporadic cases; overall, in 6 of 13 (46%) MPNSTs. Homozygous deletions of exon 2 were found in 5 of 10 (50%) NF1 cases (Fig. 3e) and 4 of 12 (33%) sporadic cases; overall, in 9 of 22 (41%) MPNSTs. Both exons 1 and 2 were deleted in two cases (Cases 2 and 20). None of the evaluable MPNSTs (16 of 26; 8 NF1 and 8 sporadic cases) had an exon 3 deletion. Of 11 neurofibromas, 8 were successfully analyzed for at least one exon of the *p16*^{INK4A} gene (Fig. 3e), and, in these cases, no homozygous deletions were found.

ICC Correlation. A null p16 immunophenotype was present in all NF1-related and -unrelated MPNSTs carrying a deletion. p16 immunoreactivity was observed in cases that did not have homozygous deletions in any of the *p16*^{INK4A} exons, with the exception of two MPNSTs (Cases 7 and 26) and two neurofibromas (Cases 2 and 15). The polyclonal antibody to p16 that we used was also tested in a comprehensive study evaluating the limitations of the ICC p16 assay, with adequate results (Geradts et al, 2000).

LOH and MSI Correlations. The analysis at 9p21 locus was successfully performed in 23 of 28 (11 NF1 and 12 sporadic) cases. LOH was found in 4 of 11 (36%) NF1-related and 3 of 12 (25%) sporadic cases (Fig. 4); overall, in 7 of 23 (30%) MPNSTs. Four cases (Cases 2, 7, 13, and 25) had both LOH at the 9p21 locus and a homozygous deletion of the *p16*^{INK4} gene (Fig. 3f). In two cases, one NF1-associated (Case 8) and one sporadic (Case 16) case, only evidence of LOH was present. Case 21, with LOH, was not evaluable for *p16*^{INK4A} analysis. In one additional case (Case 24), both homozygous deletion of the *p16*^{INK4} gene and MSI at the 9p21 locus were found. Cumulatively, evidence of homozygous deletion and/or LOH was present in 16 of 23 (69.5%) cases.

Discussion

The present study was undertaken to investigate the occurrence of possible distinct pathways of transfor-

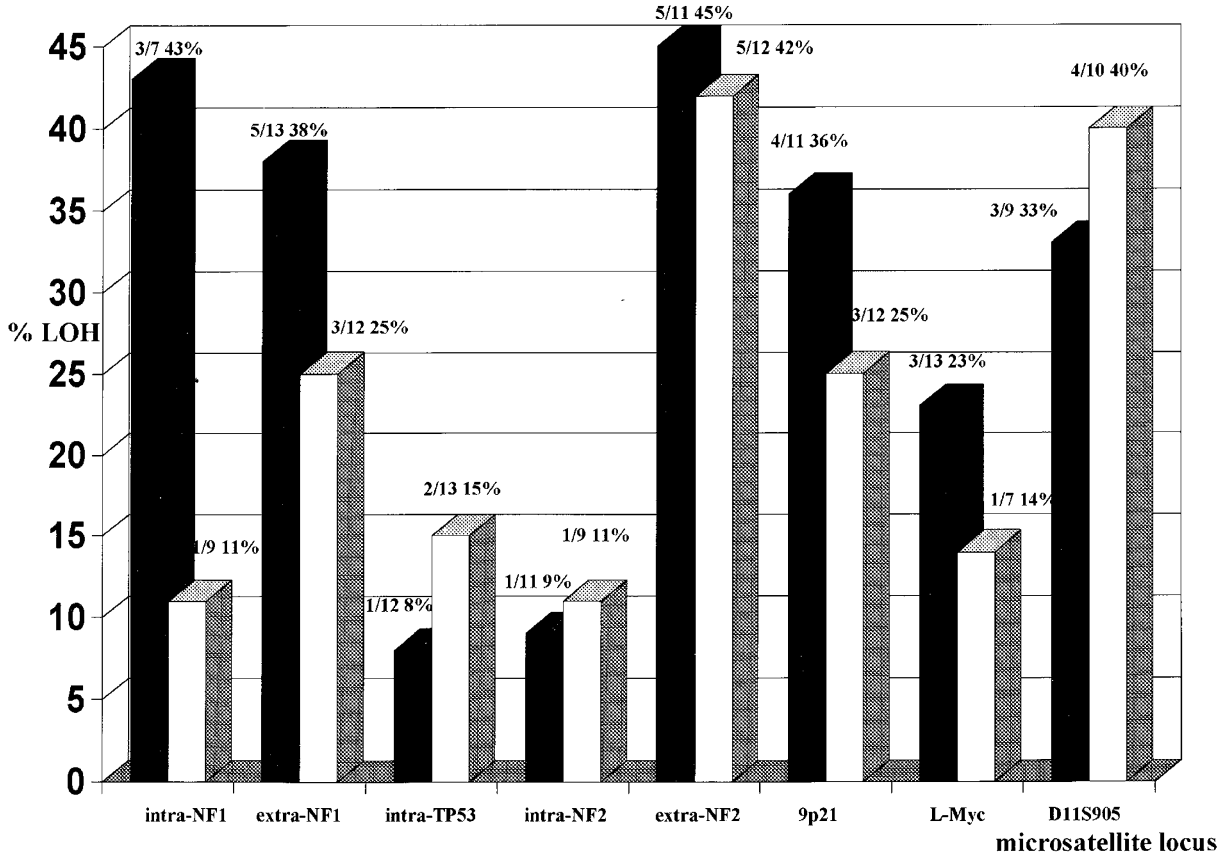

Figure 4.
Microsatellite analysis data from *NF1*-related and sporadic MPNSTs. *LOH*, loss of heterozygosity. *Filled bars*, LOH in *NF1*-related MPNSTs; *Open bars*, LOH in sporadic MPNSTs.

Table 3. Features of Selected Microsatellites

Microsatellite	Type	Locus
P53	Dinucleotide	17p13
D17S740	Dinucleotide	17p; 17 CM from NF1
IVS27AC28	Dinucleotide	17q11.2; intron 27 of NF1
IVS27TG24	Dinucleotide	17q11.2; intron 27 of NF1
CA/GT	Dinucleotide	17q11.2; intron 38 of NF1
D17S966	Tetranucleotide	17q
D17S787	Dinucleotide	17q; 17 CM from NF1
D22S430	Dinucleotide	Distal NF2
D22S275	Dinucleotide	Proximal NF2
D22S929	Dinucleotide	22q12.1; intra NF2
IFNA	Dinucleotide	9p21
D9S171	Dinucleotide	9p21
D9S126	Dinucleotide	9p21
L-Myc	Tetranucleotide	1p32
D11S905	Tetranucleotide	11q12
BAT26	Poly-A	2q; intron 5 of hMSh2

mation within subgroups of MPNSTs. Despite a superimposable histologic and cytoskeleton-based immunophenotype, the subgroups differ in clinical setting and genetic background; one subgroup is associated with NF1 genetic syndrome and the other is not.

The incidences of Rb pathway alterations, represented by either *p16*^{INK4A} gene homozygous deletion or LOH at the relative 9p21 locus, and by a null p16 immunophenotype, was 69.5% and near 100%, respectively. The incidences were almost equal between NF1-associated and sporadic MPNSTs. These results are in keeping with recent data published by two different groups (Kourea et al, 1999; Nielsen et al, 1999), and suggest a crucial role of *p16*^{INK4A} gene inactivation in malignant transformation of MPNSTs, irrespective of a familial association of the disease. The almost ubiquitous Rb expression, excluding allelic loss or mutations of the *Rb* gene, is in agreement with the inverse relationship between aberrations of p16 and Rb (Otterson et al, 1994; Ueki et al, 1996). In this context, it is expected that the observed cdk4-null immunophenotype reflects the lack of *CDK4* amplification in all but one case (Case 18) (Ichimura et al, 1996).

Evidence of a segregation of *TP53* pathway deregulation in sporadic MPNSTs is seen by separating NF1-related cases from sporadic cases. *TP53* mutations coupled with LOH at the 17p13 locus (Cases 16 and 18), and p53 overexpression not associated with *TP53* mutations or mdm2 overexpression, were 5 times (43% versus 9%), and 3 times (71% versus

25%) more frequent in sporadic cases compared with NF1 cases, respectively. In the *TP53* mutations group, we observed an uncommon redundant *TP53* gene deregulation, indicated by the presence of *TP53* mutations coupled with mdm2 immunoreactivity, which could suggest an mdm2-mediated p53 loss of function (Cases 18 and 24). As previously described (Buto et al, 1999), mdm2 overexpression may lead to a nonmutational stabilization and inactivation of the p53 protein by intermolecular complex formation. Because both of these cases carried the same type of mutation, it might be inferred that mutant Cys238Tyr does not significantly affect the overall p53 protein structure. Unfortunately, the potential functional significance of this mutation has not yet been verified.

The poor correlation between the type of p53 immunoreactivity and the type of *TP53* mutation was unexpected. No ICC reactivity was observed in four sporadic cases with *TP53* mutations; in one of these cases (Case 27), the negative ICC results could be a consequence of the appearance of a premature stop codon. Moreover, we observed strong reactivity in terms of intensity and number of immunoreactive nuclei in the absence of mutation (Cases 15, 19, 20, and 23), even extending *TP53* molecular analysis to exons 4, 9, and 10 in Cases 15 and 19, in which more than 90% of the nuclei were immunoreactive. Although we can not exclude the presence of *TP53* mutations in exons outside of the screening area, the protein accumulation in the absence of a detectable mutation suggests an altered regulation of p53 expression or the presence of unidentified p53-interacting proteins that may contribute to its stabilization. Taken together, these data suggest caution in interpreting p53 expression as a reflection of gene mutation in MPNSTs (Halling et al, 1996; Kindblom et al, 1995), and confirm that the occurrence of specific correlation patterns between genotype and immunophenotype of this gene and its related protein is highly dependent on the type of tumor examined (Donghi et al, 1993; Lavarino et al, 1998; Righetti et al, 1996).

Although the molecular mechanisms underlying tumor development in NF1 are not understood at present, it is assumed that patients with NF1 have a defect in the *NF1* gene that leads to a constitutive activation of the *RAS* oncogene through a neurofibromin loss of function mediated by the NF1 inactivation (Shen et al, 1996). In turn, the *NF1* inactivation seems to be related to an inherited germ-line mutation at one *NF1* allele followed by a somatic inactivation of the second allele (Skuse et al, 1989). Therefore, the percentage and extension of LOH detected in the present study at the 17q chromosomal region encompassing the *NF1* gene locus are consistent with a somatic inactivation of the second *NF1* allele in tumor cells.

Recent preclinical evidence suggests a causal role of *TP53* mutations in the development of MPNSTs in *NF1*-null mice (Cichowski et al, 1999; Vogel et al, 1999). However, the mouse model may or may not mirror the human one, thus, this evidence does not contradict our observations of less involvement of *TP53* alterations in NF1 cases. The abrogation of p53 activity may also be achieved through mdm2-mediated p53 degradation, a feed-back mechanism that may be inactivated by $p19^{ARF}$ overexpression (Kamijo et al, 1999). However, $p19^{ARF}$ loss of function, which may be related to the commonly found *INK4* gene deletion, could enhance an indirect p53 inactivation. Recent data report that *ARF*-null mice are highly cancer prone; sarcomas and lymphomas are the most common tumors arising spontaneously in these animals (Kamijo et al, 1999).

In some cases reported here, from both NF1-related (Case 2) and sporadic (Case 20) cases, a deletion of $p19^{ARF}$ may be envisaged. Additionally, loss of the exon 2 *INK4A* gene with a concomitant deletion of $p16^{INK4A}$ and $p19^{ARF}$ genes was reported in 60% of MPNSTs analyzed (Kourea et al, 1999), and a homozygous deletion of exon 1α coupled with exon 1β was observed in all human high-grade astrocytomas previously investigated for exon 2 of the *INK4A* gene (Newcomb et al, 2000).

In agreement with some studies (Glover et al, 1991; Menon et al, 1990) and in contrast with others (Colman et al, 1995; Ottini et al, 1995; Sawada et al, 1996; Serra et al, 1997), we did not find LOH in neurofibromas, with the exception of Case 16. In Case 16, both the benign-featuring wide re-excision performed 1 month after the surgical treatment of the primary MPNST and the malignant recurrence that developed 6 years later had the same LOH pattern at D11S905. This suggests the presence of these molecular alterations in a lesion morphologically and immunophenotypically (immunoreactive for p16) benign. Regarding the lack of LOH in the neurofibromas, we think that the high heterogeneity of cellular proliferation, the restricted number of loci investigated, the geographic differences, and the tissue fixation type could have led to an overestimation of this phenomenon as proposed by Serra et al (1997, 2000). The microsatellite data mostly agreed with the gene-based immunophenotypic profile. No marker inconsistencies were found in the cases analyzed, with the exception of two *p16*-null cases (in two neurofibromas, one plexiform in subtype and one NF1 related). It is interesting that the plexiform neurofibroma, thought to be more prone to malignant transformation and thus regarded as "atypical" biologically, had a loss of p16 immunoreactivity.

In conclusion, our differential analysis confirmed the $p16^{INK4A}$ gene deletion as a hallmark of NF1-related and sporadic MPNSTs, and highlighted a unique deregulation of the *TP53* pathway in sporadic MPNSTs. Moreover, our results confirm the concept of a somatic inactivation by LOH of the second *NF1* allele in NF1-related MPNSTs.

Materials and Methods

Patients

Three hundred cases with a diagnosis of MPNST and/or neurofibroma, surgically treated and/or cured at the National Cancer Institute of Milan from 1990 to 1998 were electronically retrieved from our data base;

28 were suitable for the present study. Exclusion criteria encompassed: (a) inadequate fixation for molecular analysis (more than 50% of cases were Bouin's fixed); (b) referred cases, ie, cases without embedded material (more than 30% of cases); (c) unsuitable lesions for wide necrotic areas or absence of normal tissue as negative control; (d) lesions of interest but previously treated with radiotherapy. Patients (Tables 1 and 2) who received chemotherapy, even before surgery, were included in the study.

The medical records of the selected cases were revised by a medical geneticist who classified cases as neurofibromatosis type I (NF1)-related or -unrelated, according to officially coded National Institutes of Health Neurofibromatosis Consensus Development Conference criteria (National Institutes of Health, 1988).

NF1 Patients

In the absence of germ-line or somatic mutation analysis of the *NF1* gene, 14 of 28 cases met the National Institutes of Health criteria. As shown in Table 1, the NF1 cases analyzed consisted of 9 females and 5 males with disease-onset ages ranging from 9 to 39 years (mean value, 20 years). There was a positive family history in two cases (Cases 1 and 6); a negative family history in two cases (Case 7 and 8); and features consistent with NF1 segmental and NF1-Noonan syndrome, respectively, in two additional cases (Cases 10 and 14). For the remaining patients, familiarity was difficult to establish.

In seven cases (Cases 1, 2, 3, 4, 10, 11, and 13) both primary malignant and benign lesions were analyzed; in four cases (Cases 5, 6, 7, and 12), only the primary malignant lesion was available; and in two cases (Cases 9 and 14), we could arrange the benign lesion only. Lastly, in one case (Case 8), we analyzed only the lung metastasis from a primary MPNST treated elsewhere. Overall, we analyzed 16 primary MPNSTs, 13 neurofibromas, and 1 metastasis from 14 NF1 patients. All primary MPNSTs but one (Case 2, G2) were high-grade sarcomas (G3), one of which was epitheloid in subtype. One of 13 neurofibromas was plexiform in subtype.

Sporadic Patients

No clinical signs of NF1 or positive family history for disease were found in the 14 sporadic cases analyzed. In some of these patients, a positive familial history for neoplasia was reported (Table 2), and Case 23 carried a *INK4A* locus deletion syndrome. The 14 sporadic cases comprised 7 females and 7 males with disease-onset ages ranging from 25 to 82 years (median, 54 years) (Table 2). We obtained suitable material from both primary malignant and benign lesions in two cases (Cases 15 and 16), and in two cases (Cases 17 and 18), we analyzed the primary tumor and a lung metastasis. In the remaining 10 cases, we analyzed the primary MPNST only. We analyzed a total of 14 primary MPNSTs, 2 neurofibromas, and 2 metastases. Eight primary MPNSTs were G3 and six were G2, two of these were epitheloid in subtype.

ICC

Immunophenotyping for p53, mdm2, p16, pRb, and cdk4 proteins was performed in all cases under study. The antibodies applied were: a monoclonal antibody (mAb) to p53 diluted 1:1000 (DO7; Novocastra, Newcastle Upon Tyme, United Kingdom); a mAb to mdm2 diluted 1:1000 (IF2; Oncogene Science, Cambridge, Massachusetts); a polyclonal antibody to p16 diluted 1:200 (PharMingen International, San Diego, California); mAbs to pRb diluted 1:200 (PMG3–245; PharMingen, Ab4; Oncogene Science); and a polyclonal antibody to cdk4 diluted 1:200 (C22; Santa Cruz Biotechnology, Santa Cruz, California). ICC was performed on formalin-fixed and paraffin-embedded material by the peroxidase-streptavidin method, as previously described (Lavarino et al, 1998). Antigen retrieval was performed by pretreating the sections at 95° C for 6 minutes in an autoclave, with the exception of cdk4 and p16, which did not receive any antigen-retrieval treatments (plain). Positive and negative controls stained adequately. Cases were regarded as immunoreactive for each marker when at least 10% of the cells had clear immunoreactivity.

Microdissection and DNA Extraction

A careful selection of malignant, benign, and nontumoral tissue, was performed by microdissection under microscope control of methylene-blue–stained sections obtained from formalin-fixed paraffin-embedded tissues. Nontumoral tissue was used for DNA controls for microsatellite analysis. DNA extraction and purification were carried out following standard procedures, proteinase K digestion and subsequent spin-column purification (QIAamp Tissue Kit; Qiagen, Valencia, California). Purified DNA was quantified by spectrophotometer (Pharmacia Biotech Ltd., Cambridge, United Kingdom) and diluted with TE at a final concentration of 50 ng/μl.

Microsatellite Markers

Sixteen polymorphic loci were selected for detection of LOH and/or MSI in MPNSTs and neurofibromas from 28 NF1-related and -unrelated cases (Table 3). Seven microsatellite markers mapped at chromosome 17 and three markers mapped at chromosome 22 were selected in regions proximal, distal, and intragenic to *TP53*, *NF1*, and *NF2*; three markers were located at chromosome 9, encompassing the *INK4A* locus; one marker was selected at chromosome 1 upstream to the *L-Myc* gene; one marker was located at chromosome 11, near the exostosis gene; and one marker (BAT26) was selected at chromosome 2q, intron 5, of the *MLH2* gene to assess the occurrence of MSI caused by mismatch repair gene defects. Primer sequences were obtained from the Genome Data Base.

Microsatellite Assay

We performed a one-step radioactive polymerase chain reaction (PCR)-based microsatellite assay for LOH and/or MSI detection at the chosen chromosomal loci, as previously described (Birindelli et al, 2000). DNA amplification was performed by an automated Thermocycle Machine (Perkin-Elmer, Foster City, California); conditions were optimized for each locus to ensure a high specificity of PCR products. For the D9S126 marker located at chromosome 9p21, we performed a nested PCR using 1 μl of PCR product as the template for the internal PCR. For the two markers located at chromosome 9p21, we performed a fluorochrome PCR-based microsatellite assay with two fluorescent dye primers: 5' ABI-Hex IFNA and 5' ABI-Ned D9S126, using the same conditions described above. The D11S905 microsatellite marker was used in some cases with both radioactive and fluorescent procedures, without obtaining contrasting results.

For the manual radioactive procedure, LOH was scored when the radiographic signal of one allele was clearly reduced in the tumor DNA compared with the corresponding normal alleles; MSI was assigned to samples that had additional bands with respect to normal alleles. In the automatic-fluorochrome assay, the fluorescence detected in the laser scanning region was collected and stored using the Data Collection software, version 2.5 (Perkin-Elmer) and gel data were automatically analyzed by the Genescan Analysis program, version 3.1 (Perkin-Elmer) at the end of the run. LOH was defined when the ratio of normal (N) and tumor (T) alleles peak height (N1:N2/T1:T2) was less than 0.5 or greater than 2. MSI was scored when peaks were detected in addition to normal alleles. Each result was confirmed at least twice and the data interpreted by two independent operators.

TP53 PCR-SSCP

All samples were screened by nested PCR-SSCP analysis for the presence of *TP53* mutations, in the most frequently affected exons (5 through 8) of the gene. In two cases (Cases 15 and 19), the *TP53* molecular investigation was extended to exons 4, 9, and 10. PCR-amplified exons with abnormal migrations were subjected to direct DNA sequencing with the Ampli Cycle Sequencing kit (Perkin-Elmer Cetus, Brachburg, New Jersey), and in some cases, to automated DNA sequencing (Perkin-Elmer Cetus). Each sequencing reaction was performed at least twice from separate amplifications, and was confirmed on sense and antisense strands. Nested PCR-SSCP analysis and direct DNA sequencing were performed as described previously (Pilotti et al, 1997).

Homozygous Deletion of $p16^{INK4}$ Gene

Homozygous deletion assay was performed by using a multiplex semi-nested comparative PCR. Each $p16^{INK4A}$ gene exon was co-amplified with a fragment of human β-*globin* gene, as previously described (Hussussian et al, 1994; Kamb et al, 1994; Saiki et al, 1988). β-*globin* gene primers (Lawn et al, 1980) were carefully selected to avoid cross-binding with $p16^{INK4A}$ primers during PCR, and the reaction conditions were optimized to $p16^{INK4A}$ gene amplification advantage. PCR products were subjected to electrophoresis through 3% to 4% agarose gels, and images were stored and analyzed with Image Master VDS software (Pharmacia Biotech). The mean ratio of $p16^{INK4A}$ and β-*globin*–fragment signal intensity was calculated for all malignant and benign samples. To evaluate possible interference of minimal normal tissue contamination, we harvested varying mixtures of tumor DNA of the 15392/90 cell line completely deleted for $p16^{INK4A}$ gene (obtained in our Institute from a melanoma patient) and normal genomic DNA (p16 wild-type control). The DNA mixtures contained percentages of normal DNA varying from 0% to 100% versus the tumor DNA counterpart. Only samples presenting a mean ratio between $p16^{INK4A}$ and β-*globin* band intensities less than the DNA mixture with 10% of normal DNA were regarded as homozygously deleted. Results suggestive of $p16^{INK4A}$ deletion were confirmed at least twice by independent reactions. Moreover, we applied the same procedure to five additional normal samples from healthy controls to evaluate the mean efficiency of the reaction.

Acknowledgement

We thank Mr. M. Azzini for photographic assistance and the Melanoma Genetic Unit for kindly providing the 15392/90 cell line.

References

Berner JM, Sorlie T, Mertens F, Henriksen J, Sater G, Mandahl N, Brogger A, Myklebost O, and Lothe RA (1999). Chromosome band 9p21 is frequently altered in malignant peripheral nerve sheath tumors: Studies of *CDKN2A* and other genes of the pRB pathway. Genes Chromosomes Cancer 26:151–160.

Birindelli S, Tragni G, Bartoli C, Ranzani G, Rilke F, Pierotti MA, and Pilotti S (2000). Detection of microsatellite alterations in the spectrum of melanocytic nevi in patients with or without individual or family history of melanoma. Int J Cancer 86:255–261.

Buto S, Pierotti MA, Tamborini E, Della Torre G, Lavarino C, Rilke F, and Pilotti S (1999). Biochemical uncovering of mdm2/p53 complexes in liposarcomas parallels their immunohistochemical detection. Diagn Mol Pathol 8:125–130.

Cho YL, Gorina S, Jeffrey PD, and Pavletich NP (1994). Crystal structure of a p53 tumor suppressor-DNA complex: Understanding tumorigenic mutations. Science 265:346–355.

Cichowski K, Shih TS, Schmitt E, Santiago S, Reilly K, McLaughlin ME, Bronson RT, and Jacks T (1999). Mouse models of tumor development in neurofibromatosis type 1. Science 286:2172–2176.

Colman SD, Williams CA, and Wallace MR (1995). Benign neurofibromas in type 1 neurofibromatosis (*NF1*) show somatic deletions of the *NF1* gene. Nat Genet 11:90–92.

Donghi R, Longoni A, Pilotti S, Michieli P, Della Porta G, and Pierotti MA (1993). Gene *p53* mutations are restricted to poorly differentiated and undifferentiated carcinomas of the thyroid gland. J Clin Invest 91:1753–1760.

Ducataman BS, Scheithauer BW, Piepgras DG, Reiman HM, and Ilstrup DM (1986). Malignant peripheral nerve sheath tumors. Cancer 57:2006–2021.

Fletcher CDM, Dal Cin P, de Wever I, Mandahl N, Mertens F, Mitelman F, Rosai J, Rydholm A, Sciot R, Tallini G, van den Berghe H, Vanni R, and Willen H (1999). Correlation between clinicopathological features and karyotype in spindle cell sarcomas. Am J Pathol 154:1841–1847.

Geradts J, Hruban RH, Schutte M, Kern S, and Maynard R (2000). Immunohistochemical $p16^{INK4a}$ analysis of archival tumors with deletion, hypermethylation, or mutation of the CDKN2/MTS1 gene. A comparison of four commercial antibodies. Appl Immunohistochem Molecul Morphol 8:71–79.

Glover TW, Stein CK, Legius E, Andersen LB, Brereton A, and Johnson S (1991). Molecular and cytogenetic analysis of tumors in von Recklinghausen neurofibromatosis. Genes Chromosomes Cancer 3:62–70.

Greenblatt MS, Bennett WP, Hollstein M, and Harris CC (1994). Mutations in *p53* tumor suppressor gene: Clues to cancer etiology and molecular pathogenesis. Cancer Res 54:4855–4878.

Halling KC, Scheithauer BW, Halling AC, Nascimento AG, Ziesmer SC, Roche PC, and Wollan PC (1996). p53 expression in neurofibroma and malignant peripheral nerve sheath tumor. Am J Clin Pathol 106:282–288.

Hussussian CJ, Struewing JP, Goldstein AM, Higgins PAT, Ally DS, Sheahan MD, Clark WH Jr, Tucker MA, and Dracopoli NC (1994). Germline p16 mutations in familial melanoma. Nat Genet 8:15–21.

Ichimura K, Schmidt EE, Goike HG, and Collins P (1996). Human glioblastomas with no alterations of the *CDKN2A* ($p16^{INK4A}$, *MTS1*) and *CDK4* genes have frequent mutations of the retinoblastoma gene. Oncogene 13:1065–1072.

Kamb A, Shattuck-Eidens D, Eeles R, Liu Q, Gruis NA, Ding W, Hussey C, Tran T, Miki Y, Weaver-Feldhaus J, McClure M, Aitken F, Anderson DE, Bergman W, Frants R, Goldgar DE, Green A, MacLennan R, Martin NG, Meyer LJ, Youl P, Zone JJ, Skolnick MH, and Cannon-Albright LA (1994). Analysis of the *p16* gene (*CDKN2*) as a candidate for the chromosome 9p melanoma susceptibility locus. Nat Genet 8:22–26.

Kamijo T, Bodner S, van de Kamp E, Randle DH, and Sherr CJ (1999). Tumor spectrum in *ARF*-deficient mice. Cancer Res 59:2217–2222.

Kindblom L-G, Ahlden M, Meis-Kindblom JM, and Stenman G (1995). Immunohistochemical and molecular analysis of p53, proliferating cell nuclear antigen and ki67 in benign and malignant peripheral nerve sheath tumours. Virchows Arch 427:19–26.

Kourea HP, Orlow I, Scheithauer BW, Cordon-Cardo C, and Woodruff JM (1999). Deletions of the *INK4A* gene occur in malignant peripheral nerve sheath tumors but not in neurofibromas. Am J Pathol 155:1855–1860.

Lavarino C, Corletto V, Mezzelani A, Della Torre G, Bartoli C, Riva C, Pierotti MA, Rilke F, and Pilotti S (1998). Detection of *TP53* mutation, loss of heterozygosity and DNA content in fine-needle aspirates of breast carcinoma. Br J Cancer 77:125–130.

Lawn RM, Efstratiadis A, O'Connell C, and Maniatis T (1980). The nucleotide sequence of the human *β-globin* gene. Cell 21:647–651.

Legius E, Dierick H, Wu R, Hall BK, Marynen P, Cassiman JJ, and Glover W (1994). *TP53* mutations are frequent in malignant *NF1* tumors. Genes Chromosomes Cancer 10:250–255.

May P and May E (1999). Twenty years of p53 research: Structural and functional aspects of the p53 protein. Oncogene 18:7621–7636.

Mechtersheimer G, Otano-Joos M, Ohl S, Benner A, Lehnert T, Willeke F, Moller P, Otto H, Lichter P, and Joos S (1999). Analysis of chromosomal imbalances in sporadic and *NF1*-associated peripheral nerve sheath tumors by comparative genomic hybridization. Genes Chromosomes Cancer 25: 362–369.

Menon AG, Anderson KM, Riccardi VM, Chung RY, Whaley JM, Ledbetter DH, Kleider A, Martuza R, Gusella JF, and Seizinger BR (1990). Chromosome 17p deletions and *p53* gene mutations associated with the formation of malignant neurofibrosarcomas in von Recklinghausen neurofibromatosis. Proc Natl Acad Sci USA 87:5435–5439.

National Institutes of Health (1988). Neurofibromatosis. Conference statement. National Institutes of Health Consensus Development Conference. Arch Neurol 45:575–578.

Newcomb EW, Alonso M, Sung T, and Miller DC (2000). Incidence of *p14ARF* gene deletion in high-grade adult and pediatric astrocytomas. Hum Pathol 31:115–119.

Nielsen GP, Stemmer-Rachamimov AO, Ino Y, Moller MB, Rosenberg AE, and Louis DN (1999). Malignant transformation of neurofibromas in neurofibromatosis 1 is associated with *CDKN2A/p16* inactivation. Am J Pathol 155:1879–1884.

Otterson GA, Kratzke RA, Coxon A, Kim YW, and Kaye FJ (1994). Absence of p16INK4 protein is restricted to the subset of lung cancer lines that retains wildtype RB. Oncogene 9:3375–3378.

Ottini L, Esposito DL, Richetta A, Carlesimo M, Palmirotta R, Veri MC, Battista P, Frati L, Caramia FG, Calvieri S, Cama A, and Mariani-Costantini R (1995). Alterations of microsatellite in neurofibromas of von Reckinghausen's disease. Cancer Res 55:5677–5680.

Pilotti S, Della Torre G, Lavarino C, Di Palma S, Sozzi G, Minoletti F, Rao S, Pasquini G, Azzarelli A, Rilke F, and Pierotti MA (1997). Distinct mdm2/p53 expression patterns in liposarcoma subgroups: Implications for different pathogenetic mechanisms. J Pathol 181:14–24.

Poyhonen M, Niemela S, and Herva R (1997). Risk of malignancy and death in neurofibromatosis. Arch Pathol Lab Med 121:139–143.

Prives C (1994). How loops, β sheets and α helices help us to understand p53. Cell 78:543–546.

Righetti SC, Della Torre G, Pilotti S, Ménard S, Ottone F, Colnaghi M, Pierotti MA, Lavarino C, Cornarotti M, Oriana S, Böhm S, Bresciani GL, Spatti G, and Zunino F (1996). A comparative study of *p53* gene mutations, protein accumulation, and response to cisplatin-based chemotherapy in advanced ovarian carcinoma. Cancer Res 56:689–693.

Saiki RK, Gelfand DH, Stoffel S, Scharf SJ, Higuchi R, Horn GT, Mullis KB, and Erlich HA (1988). Primer-directed enzymatic amplification of DNA with a thermostable DNA polymerase. Science 239:487–491.

Sawada S, Florell S, Purandare SM, Ota M, Stephens K, and Viskochil D (1996). Identification of *NF1* mutations in both alleles of a dermal neurofibroma. Nat Genet 14:110–112.

Serra E, Puig S, Otero D, Gaona A, Kruyer H, Ars E, Estivill X, and Lazaro C (1997). Confirmation of a double-hit model for the *NF1* gene in benign neurofibromas. Am J Hum Genet 61:512–519.

Serra E, Rosenbaum T, Winner U, Aledo R, Ars E, Estivill X, Lenard H-G, and Lazaro C (2000). Schwann cells harbor the somatic *NF1* mutation in neurofibromas: Evidence of two different Schwann cell subpopulations. Hum Mol Genet 9:3055–3064.

Shen MH, Harper PS, and Upadhyaya M (1996). Molecular genetics of neurofibromatosis type 1 (*NF1*). J Med Genet 33:2–17.

Skuse GR, Kosciolek BA, and Rowley PT (1989). Molecular genetic analysis of tumors in von Recklinghausen neurofibromatosis: Loss of heterozygosity for chromosome 17. Genes Chromosomes Cancer 1:36–41.

Vogel KS, Klesse LJ, Velasco-Miguel S, Meyers K, Rushing EJ, and Parada LF (1999). Mouse tumor model for neurofibromatosis type 1. Science 286:2176–2179.

Ueki K, Ono Y, Henson JW, Efird JT, von Deimling A, and Louis DN (1996). *CDKN2/p16* or *RB* alterations occur in the majority of glioblastomas and are inversely correlated. Cancer Res 56:150–153.